Structural and magnetic properties of the oxyborate $Co_5Ti(O_2BO_3)_2$

D. C. Freitas, R. B. Guimarães, D. R. Sanchez, and J. C. Fernandes
Instituto de Física, Universidade Federal Fluminense, Campus da Praia Vermelha, 24210-346 Niterói, RJ, Brazil

M. A. Continentino*
Centro Brasileiro de Pesquisas Físicas, Rua Dr. Xavier Sigaud 150, Urca, 22290-180 Rio de Janeiro, RJ, Brazil

J. Ellena
Instituto de Física de São Carlos, Universidade de São Paulo, Caixa Postal 369, 13560-970 São Carlos, SP, Brazil

A. Kitada and H. Kageyama
Department of Chemistry, Graduate School of Science, Kyoto University, Sakyo, Kyoto 606-8502, Japan

A. Matsuo and K. Kindo
Institute for Solid State Physics, University of Tokyo, Kashiwa, Chiba 277-8581, Japan

G. G. Eslava and L. Ghivelder
Instituto de Física, Universidade Federal do Rio de Janeiro, Caixa Postal 68528, 21945-970 Rio de Janeiro, RJ, Brazil
(Received 16 October 2009; revised manuscript received 8 January 2010; published 29 January 2010)

We present an extensive study of the oxyborate material $Co_5Ti(O_2BO_3)_2$ using x-ray, magnetic, and thermodynamic measurements. This material belongs to a family of oxyborates known as ludwigites which presents low-dimensional subunits in the form of three leg ladders in its structure. Differently from previously investigated ludwigites the present material does not show long-range magnetic order although it goes into a spin-glass state at low temperatures. The different techniques employed in this paper allow for a characterization of the structure, the nature of the low-energy excitations and the magnetic anisotropy of this system. Its unique magnetic behavior is discussed and compared with those of other magnetic ludwigites.

DOI: 10.1103/PhysRevB.81.024432 PACS number(s): 75.50.−y, 73.50.Fq, 75.40.−s, 75.30.Gw

I. INTRODUCTION

Some anhydrous cobalt oxyborates adopting the ludwigite-type structure have recently been studied from the magnetic and structural point of view. Among these we mention $Co_3O_2BO_3$,[1,2] $Co_2FeO_2BO_3$,[3] and $Co_{3-x}Fe_xO_2BO_3$.[4] These studies were stimulated mainly by the singular physical properties found in the homometallic ludwigite type or vonsenite $Fe_3O_2BO_3$.[5–9] As a trial for better understanding the complex magnetic behavior of all these materials we decided to extend this work and to study a cobalt ludwigite-type compound containing nonmagnetic ions. In this way we synthesized the ludwigite $Co_5Ti(O_2BO_3)_2$ and measured its ac susceptibility, magnetization, and specific heat between 2 K and room temperature (RT). X-ray diffraction in single crystals at RT and 150 K, as well as magnetization under pulsed applied fields up to 55 T were also measured. The present work reports the results of such measurements and discusses them in comparison with those obtained for the above mentioned, previously investigated cobalt ludwigites.

II. SAMPLES

A. Synthesis

The crystals were synthesized from a 6:1:3:6 molar mixture of $CoO:Li_2TiO_3:HBO_3:Na_2B_4O_7$. The mixture was fired at 1100 °C for 24 h and cooled down to 600 °C for 48 h. Than the oven was turned off. The bath was dissolved in hot water and the crystals washed in diluted cold hydrochloric acid. Needle-shaped black crystals up to 4 mm in length were obtained.

B. X-ray diffraction

A prism-shaped crystal was employed for data collection from x-ray diffraction. The measurements were carried out on an Enraf-Nonius Kappa-CCD diffractometer with graphite monochromated Mo $K\alpha$ radiation ($\lambda=0.71073$ Å). Low-temperature measurements were made using an Oxford Cryosystem device. The cell refinements were performed using the softwares COLLECT (Ref. 10) and SCALEPACK.[11] The final cell parameters were obtained on all reflections. Data were collected up to 62.0° in 2θ. Data reduction was carried out using the softwares, DENZO-SMN, SCALEPACK, and XDISPLAYF (Ref. 11) for visual representation of data. Gaussian absorption correction was applied.[12] The structure was solved using the software SHELXS-97 (Ref. 13) and refined using the software SHELXL-97.[14] The tables were generated by WINGX.[15] All atoms were clearly solved and least-squares refinement procedures on F^2 with anisotropic thermal parameters were carried on using SHELXL-97. Crystal data, data collection parameters and structure refinement data are summarized in Table I.

We decided to resolve the structure at 293 and 150 K, in analogous experimental conditions, in order to observe any

TABLE I. Crystal data and structure refinement of $Co_5Ti(O_2BO_3)_2$.

Empirical formula from x-ray analysis	$Co_{9.48}Ti_{2.52}B_4O_{20}$	
Formula weight	1042.60	
Wavelength	0.717073 Å	
Crystal Size	$0.038\times0.047\times0.228$ mm^3	
Temperature	293 K	150 K
Crystal system	Orthorhombic	Orthorhombic
Space group	(No. 55) *Pbam*	(No. 55) *Pbam*
Unit cell dimension a=	9.3300(14) Å	9.3215(5) Å
b=	12.2541(11) Å	12.2522(5) Å
c=	3.0424(3) Å	3.0440(2) Å
Volume	347.84(7) Å^3	347.63(3) Å^3
Z	1	1
Density (calculated)	4.977 Mg/m^3	4.980 Mg/m^3
Absorption coefficient	12.471/mm	12.478/mm
F(000)	491	491
θ range (deg)	3.32–31.00	3.31–32.19
Index range h=	−13, 13	−13, 13
k=	−17, 14	−18, 18
l=	−4, 4	−4, 4
Reflections collected	2956	3215
Independent reflections	647	688
R(int)	0.0482	0.0635
Completeness to θ=31.00	99.8%	(32.19) 96.0%
Absorption correction	Gaussian	Gaussian
Max./min. transmission	0.6353/0.1616	0.6485/0.1236
Refinement method: full-matrix least squares on F^2		
Data/restraints/parameters	647/0/60	688/0/65
Goodness of fit on F^2	1.205	1.128
Final R indices [$I>2\sigma(I)$]	R1=0.0275	R1=0.0342
	wR2=0.0677	wR2=0.0797
R indices (all data)	R1=0.0314	R1=0.0400
	wR2=0.0690	wR2=0.0823
Extinction coefficient	0.036(3)	0.044(4)
Largest diff. peak	0.964×10^{-3} Å	0.989×10^{-3} Å
Largest diff. hole	-1.329×10^{-3} Å	-1.421×10^{-3} Å

eventual conformational change with temperature. This has been done for other oxyborates.[1,3,7] No evidence for any phase transition was found.

Figure 1 shows a schematic structure of the ludwigites projected along the c axis together with the polyhedra centered at metal ions. We remark that the complete structure, exception for the boron ions, may be obtained from the two three leg-ladders subunits formed, respectively, by the metal sites 4-2-4 and 3-1-3. These ladders are shown in details in Fig. 2. As a result of our x-ray analysis we found that sites 4 in the titanium-cobalt ludwigite are almost equally occupied by Ti and Co ions in a disordered way as in natural[17] or synthetic[18,19] titanium containing nickel ludwigites. The metal sites 1 are also occupied by Ti and Co ions in a proportion of 0.075:0.175. These occupancies factors give the best refinement for this compound. Supposing the presence of titanium ions in site 3 the refinement is unstable no matter the occupancies of the other sites. For titanium in site 2 the anisotropic displacement parameters become unacceptably large. So the chemical composition of our sample, obtained from x-ray analysis, is $Co_{4.74}Ti_{1.26}(O_2BO_3)_2$. The bond lengths in this compound are shown in Table II. The bond angles O-M-O nearest to 180° are specified for each metal site in Table III. The mean B-O bond length and the mean O-B-O bond angle are in good agreement with the expected trigonal planar geometry. Table IV shows the fractional co-

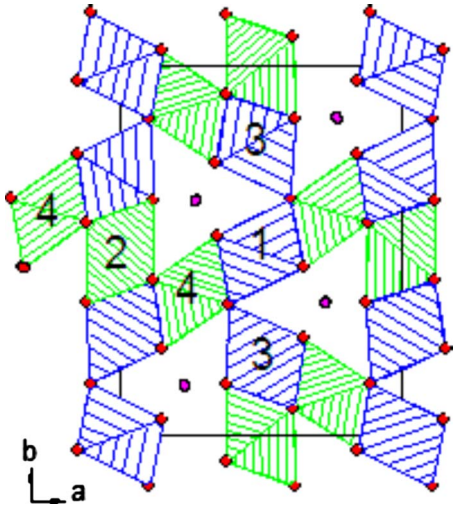

FIG. 1. (Color online) The schematic structure of the ludwigites projected along the *c* axis. The oxygen polyhedra centered on the metal ions are shown. The numbers indicate metallic sites and the lines indicate the *a* and *b* axes of the unit cell. The subunits formed by the octahedra around sites 4-2-4 and 3-1-3 are shown in more detail in Fig. 2. The boron ions (purple spheres) have trigonal coordination. This figure was generated by DIAMOND 2.1E software (Ref. 16).

ordinates and the sites occupation factor (SOF). We remark that the atomic distances and the bond angles are very similar to those of the other cobalt[1,3] and iron[7,9] ludwigitelike structures.

III. MAGNETIC MEASUREMENTS

The magnetic measurements in oriented crystals and in powdered samples of $Co_{4.74}Ti_{1.26}(O_2BO_3)_2$ [hereafter denominated $Co_5Ti(O_2BO_3)_2$] were carried out using a SQUID *MPMS, Quantum Design* equipment over the field range −7 to +7 T at 2 K. The ac magnetic susceptibility in random oriented crystals and the specific heat of this compound were measured using a commercial *PPMS platform Quantum Design*. High-field magnetization measurements up to 55 T were conducted using a pulsed magnet.

Figure 3 shows the magnetization versus temperature curves for field-cooled and zero-field-cooled (zfc) procedures, for the applied field parallel and perpendicular to the *c* axis of a single crystal. In the bottom inset a zoom of the magnetization for the first orientation is shown. The *c*-axis direction is the same as that of the needles length and is the hard axis of magnetization. In the top inset of this figure appears the inverse of magnetization in the zfc regimen for the applied field perpendicular to the *c* axis. We remark that the straight line which fits the high-temperature segment of this curve crosses the temperature axis very near the origin. This suggests that at the temperature of ≈19 K, at which the zfc magnetization curve shows a peak, the system enters a spin-glass state. This hypothesis is also supported by the frequency dependence of the real part of the ac susceptibility and by the absence of any feature in the specific-heat curve

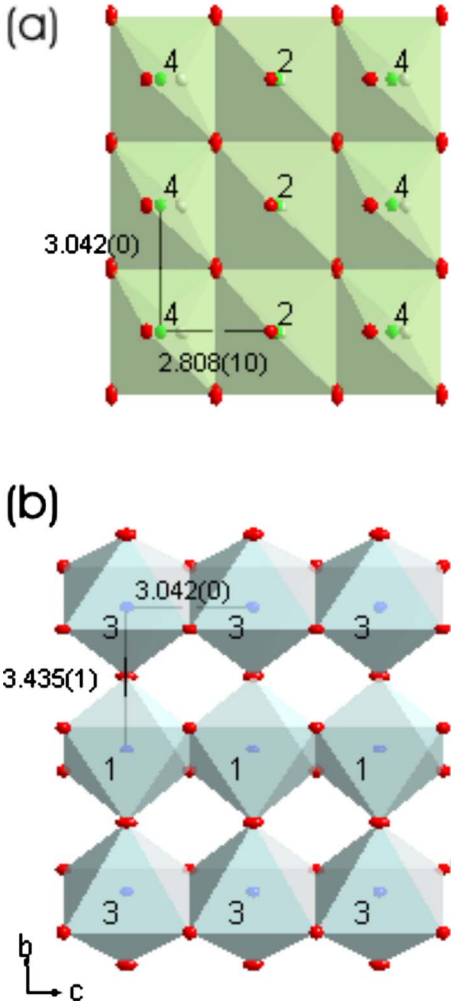

FIG. 2. (Color online) (a) The subunit formed by the metal sites 4-2-4 in which the oxygen octahedra share one edge. All the oxygen ions are out of the figure plane with the exception of four of them around the site 2. The vertical axis is the *c* axis. (b) The subunit formed by the metal sites 3-1-3 in which the oxygen octahedra around adjacent sites 1 and 3 share one corner. Notice that oxygen ions in the common corners of a column are not on the same straight line. Both subunits we call three leg ladders. This figure was generated by DIAMOND 2.1E software (Ref. 16).

[see Figs. 4(a) and 6]. Below 19 K the magnetization versus field curves present hysteresis cycles down to the lowest reached temperatures and, near 3 K, these curves present jumps. If the applied field is orthogonal to the *c* axis the hysteresis shows a null coercive field indicating that the magnetic anisotropy is negligible in the *ab* plane (see Fig. 5). Both features are compatible with a spin-glass phase.[21] The saturation of the magnetization at high applied fields indicates a magnetic moment very near $1\mu_B$ per cobalt ion, which implies a low spin state for this ion. This is the first time that a low spin state is observed in an oxyborate. Finally, the inset of Fig. 5 shows the high-field magnetization data at $T=4.2$ K for a powder sample in pulsed magnetic fields up to 55 T. This curve changes slope at ≈20 T. This type of *metamagneticlike* transition is most probably related to the field required to take the spins off the easy plane in the

TABLE II. Selected bond lengths in Å for $Co_{4.74}Ti_{1.26}(O_2BO_3)_2$. The underline numbers are the symmetry codes: (i) $x,y,z+1$; (ii) $x,y,z-1$; (iii) $-x+2,-y+2,-z+1$; (iv) $-x+1,-y+2,-z+1$; (v) $-x+3/2,y+1/2,z$; (vi) $-x+3/2,y-1/2,z$; (vii) $x+1/2,-y+3/2,-z+1$; and (viii) $x-1/2,-y+3/2,-z+1$.

Co1-O1$_{ii}$	2.035(2)	Co4-O4$_{v}$	2.069(7)
Co1-O2	2.1548(15)	B-O2	1.365(4)
Co2-O4$_{v}$	2.1073(16)	B-O3	1.388(4)
Co2-O5	2.060(2)	B-O5	1.377(4)
Co3-O1$_{iii}$	1.969(2)	Co1-Ti1$_{i}$	3.0424(3)
Co3-O3	2.1666(16)	Co1-Ti4	3.054(14)
Co3-O4$_{i}$	2.062(2)	Co2-Co4$_{iv}$	2.808(11)
Co3-O5$_{vii}$	2.1502(16)	Co3-Ti4$_{vi}$	3.125(13)
Co4-O1	1.975(7)	Co4-Ti1$_{i}$	3.027(9)
Co4-O2	2.061(12)	Co4-Ti4$_{i}$	3.0428(6)
Co4-O3$_{v}$	2.091(12)		

powdered material. The magnetization of the powder is not yet saturated even at these high fields and low temperatures. In crystalline needles the saturation magnetization should reach the value of 20 μ_B/f.u. which corresponds to the spin moment added to the $15\mu_B$ of the cobalt ions orbital moment.

IV. SPECIFIC-HEAT MEASUREMENTS

Specific-heat measurements as a function of temperature and magnetic field were performed employing 8.5 mg of randomly oriented crystalline needles. Results are shown in Figs. 6–8. For comparison we added in Fig. 6 previous results on other previously studied cobalt ludwigites. No sharp feature is observed in the specific-heat curve of the $Co_5Ti(O_2BO_3)_2$ investigated in this study apparently ruling out any phase transition. It may also be noticed that the specific-heat values of the $Co_5Ti(O_2BO_3)_2$ ludwigite are striking larger than those of the other cobalt ludwigites shown in Fig. 6. Figure 7 shows the magnetic field dependence of the specific heat. For the previously studied ludwigites this dependence was within the error bars of the experiments for the same values of the applied field. In the inset of Fig. 7 we show the differences between the measured specific heat in zero and finite magnetic field, $(C/T)_H-(C/T)_{H=0}$. In Fig. 8 the low-temperature specific heat is plotted as C/T versus T^2. In spite of the insulating character of this material, $Co_5Ti(O_2BO_3)_2$ has a non-negligible linear temperature-dependent term in the specific heat. The values of the coefficient of this term, as well as, that of the T^3 contribution are given in the figure for different values of the external magnetic field (see also Table V).

TABLE III. The largest O-M-O bond angles in degrees for $Co_{4.74}Ti_{1.26}(O_2BO_3)_2$. The underline numbers are the symmetry codes (see Table II caption).

O1$_{ii}$-Co1-O1$_{iii}$	180.000(1)
O2$_{v}$-Co1-O2$_{viii}$	180.00(12)
O4$_{ii}$-Co2-O4$_{iii}$	180.0
O5$_{iv}$-Co2-O5	180.0
O1$_{ii}$-Co3-O4$_{iii}$	179.72(9)
O5$_{viii}$-Co3-O3$_{ii}$	166.08(9)
O1$_{ii}$-Co4-O4$_{v}$	176.9(5)
O2-Co4-O3$_{v}$	174.5(6)

TABLE IV. Fractional coordinates, SOF, and the equivalent isotropic displacement parameters ($Å^2\times10^3$) for $Co_{4.74}Ti_{1.26}(O_2BO_3)_2$. U(eq) is defined as one third of the trace of the orthogonalized U_{ij} tensor. The SOF values must be multiplied by the factor 8 in order to obtain the number of atoms in the unit cell (Ref. 20).

Site	x/a	y/b	z/c	SOF	U(eq)
Co(1)	1	1	0	0.175	7(1)
Ti(1)	1	1	0	0.075	13(4)
Co(2)	1/2	1	1/2	1/4	7(1)
Co(3)	0.9982(1)	0.7197(1)	0	1/2	9(2)
Co(4)	0.7619(11)	1.1129(9)	1/2	0.26	9(1)
Ti(4)	0.7614(16)	1.1170(14)	1/2	0.24	8(1)
O(1)	0.8907(3)	1.1437(2)	1	1/2	13(1)
O(2)	0.8463(2)	0.9575(3)	1/2	1/2	10(1)
O(3)	0.8432(2)	0.7636(2)	1/2	1/2	10(1)
O(4)	0.8809(2)	0.5771(2)	1	1/2	13(1)
O(5)	0.6227(2)	0.8602(2)	1/2	1/2	9(1)
B	0.7703(4)	0.8623(3)	1/2	1/2	8(1)

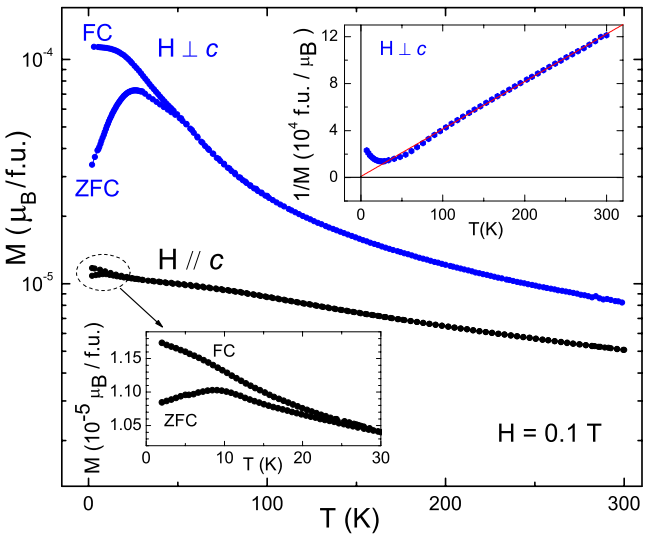

FIG. 3. (Color online) Magnetization versus temperature for crystalline needles of $Co_5Ti(O_2BO_3)_2$ under an applied field of 0.1 T in both regimens: field cooled and zero field cooled. The top inset shows the inverse of the zero-field-cooled magnetization curve for the applied field perpendicular to the c axis. The bottom inset shows a zoom of the magnetization curves for the applied field parallel to the c axis.

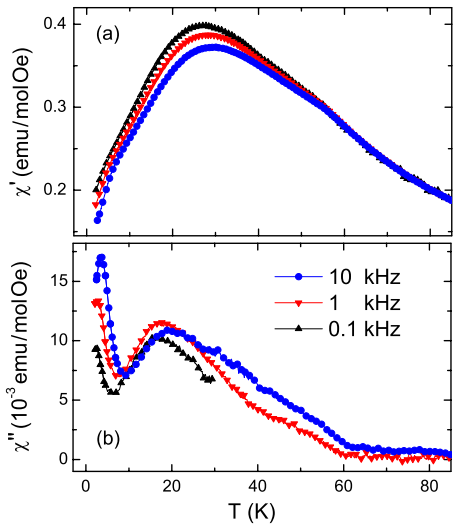

FIG. 4. (Color online) (a) Real part of the $Co_5Ti(O_2BO_3$ ac magnetic susceptibility curve as a function of the temperature for 0.1, 1, and 10 kHz. (b) Imaginary part of the same ac magnetic susceptibility for the same frequencies.

V. DISCUSSION

The results of x-ray, magnetic, and thermodynamic experiments on the $Co_5Ti(O_2BO_3)_2$ ludwigite reported here provide a quite complete characterization of this material. Besides, a comparison of these results with those on other compounds with the same structure allows for a better understanding of the physical properties of magnetic ludwigites. As we pointed out before, this is a different study of a cobalt disordered heterometallic ludwigite diluted with a nonmagnetic element, the Ti^{4+} ion. Our previous studies on the Co-Fe and Ni-Fe systems[3] have shown that the presence of different magnetic ions alone was not sufficient to destroy long-range magnetic order at low temperatures. However the substitution of the iron by a nonmagnetic component gives rise to a different behavior in that no sharp transition is observed neither in the magnetic susceptibility nor in the specific-heat experiments. On the contrary we find clear evidence for a freezing of the magnetic moments in a spin-glass

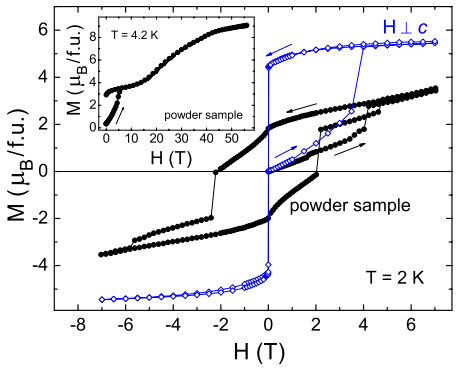

FIG. 5. (Color online) $Co_5Ti(O_2BO_3)_2$ magnetization curve versus applied field at 2 K for a powdered sample and a crystalline needle. The inset shows magnetization versus applied field curves for pulsed fields up to 55 T at T=4.2 K on powdered samples.

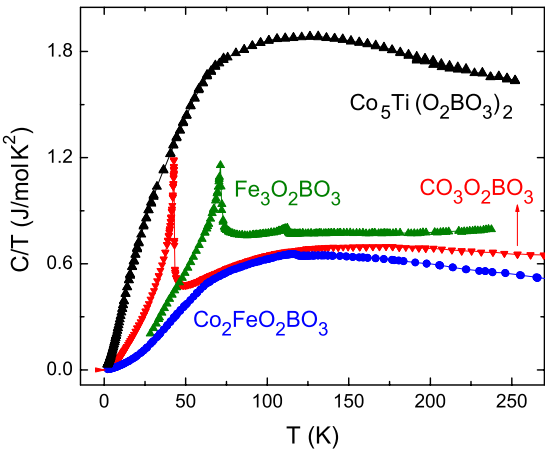

FIG. 6. (Color online) $Co_5Ti(O_2BO_3)_2$ specific heat plotted as the C/T versus T. The other specific-heat curves appearing in this figure were taken from Refs. 1, 3, and 6.

state below $T_g \approx 19$ K. This is shown here by different experiments: the high-temperature susceptibility follows a Curie-Weiss law with a paramagnetic Curie temperature θ_p, which is very close to zero (inset of Fig. 3). The dc magnetization shows a pronounced difference between field-cooled and zero-field-cooled behavior (Fig. 3), while the real part of the ac magnetic susceptibility has maxima at frequency-dependent temperatures (Fig. 4). The major evidence that our system undergoes a spin freezing phenomena at low temperatures and not a true phase transition to a magnetically long-range-ordered ground state is provided by the specific-heat measurements. As can be seen in Fig. 6, differently from previous studies in magnetic ludwigites, the specific-heat curve of $Co_5Ti(O_2BO_3)_2$ shows only a broad maximum when plotted as C/T as a function of temperature. The existence of a spin-glass transition in $Co_5Ti(O_2BO_3)_2$ is also consistent with the opening of hysteresis loops in the magnetization below T_g (see Fig. 5). At low temperatures the magnetization presents jumps as the external magnetic field is varied. Figure 5 shows also the magnetization curve at 2 K

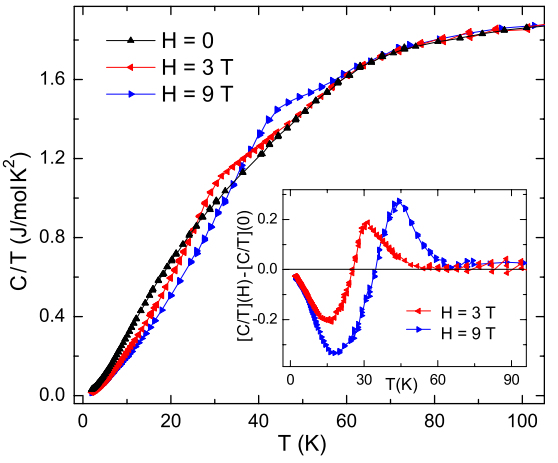

FIG. 7. (Color online) $Co_5Ti(O_2BO_3)_2$ specific heat plotted as C/T versus T for applied fields of 0, 3, and 9 T. The inset shows the differential C/T versus T curve referred to T=0.

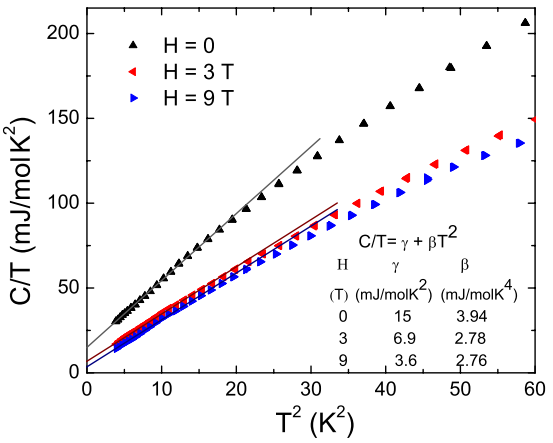

FIG. 8. (Color online) $Co_5Ti(O_2BO_3)_2$ specific heat plotted as C/T versus T^2 for applied fields of 0, 3, and 9 T. The linear behavior below approximately 10 K shows that the curves can be described by the equation $C/T=\gamma+\beta T^2$. The values of γ and β obtained from the fits are also given in the figure.

in an oriented needle with the magnetic field along the easy *ab* plane. The magnetization saturates at a value which corresponds to a magnetic moment per (chemical) formula unit of $5.5\mu_B$ and has only a small reduction when the field is turned off. More interesting there is no area in the magnetization loop in this case, which implies a negligible anisotropy along the *ab* plane. The moment of 5.5 μ_B/f.u. compares reasonably with that obtained from the high-temperature Curie-Weiss susceptibility shown in Fig. 3. If we write in this case the magnetization as $M=CH/(T-\theta_p)$, the quantity $C=N(p\mu_B)^2/(3k_B)$, where p is the number of effective Bohr magnetons. We obtain $p=4.9\pm0.2$ for fields ranging from 0.1 to 1 T. Then our magnetization results in $Co_5Ti(O_2BO_3)_2$ show not only a freezing of the moments at low temperatures, but that this freezing takes place along the *ab* plane. Along this plane there is no anisotropy and all directions are equivalent as implied by the completely reversible magnetization loop in an oriented needle. The random orientation of the moment in this plane must arrive from frustration arising from the competition of the different superexchange paths which connect different pairs of Co ions as can be seen in Figs. 1 and 2. The magnitude of the moment of ≈ 5 μ_B/f.u. is obtained assuming that the Co^{2+} ions

TABLE V. The γ and β parameters obtained for the linear fit $C/T=\gamma+\beta T^2$ of the low-temperatures extremity of the specific-heat measurements. From the β coefficient we can extract the effective Debye temperature θ_D, using $\theta_D^3=234R/\beta$, where R is the universal constant gas. H is the applied field and pw means present work.

	H (T)	γ (mJ/mol K^2)	β (mJ/mol K^4)	θ_D (K)	Ref.
$Co_3O_2BO_3$	0	3.30	0.72	139	1
$Co_2FeO_2BO_3$	0	3.28	0.23	204	3
$Co_5Ti(O_2BO_3)_2$	0	15.03	3.94	79	pw
$Co_5Ti(O_2BO_3)_2$	3	6.88	2.78	89	pw
$Co_5Ti(O_2BO_3)_2$	9	3.61	2.76	89	pw

are in a low spin state with $S=1/2$ and that their orbital angular momenta are almost completely quenched in the easy plane. On the other hand if the orbital angular momentum out of the easy plane attains its maximum value, the total magnetization could reach 20 μ_B/f.u. for a fully polarized sample since the total orbital angular momentum of the five cobalt ions in the formula unit should be added to the spin magnetization. The experimental value of $9\mu_B$ found in Fig. 5 may be due to the randomly oriented powder sample. Even the high magnetic fields and the low temperatures of these experiments are not sufficient to saturate the out-of-plane component of the magnetization.

We can see in Fig. 6 that the magnitude of the specific heat of the present sample is much larger than that of the other magnetic cobalt compounds also shown in this figure. At low temperatures this is reflected by the large γ and β values of the specific heat described by $C/T=\gamma+\beta T^2$ at these temperatures. The large β is associated with a very small Debye temperature for this oxyborate. The large γ values in the insulating ludwigites can be attributed to magnetic frustration in these materials. An inspection of their structure in Figs. 1 and 2 shows that there are many superexchange paths which lead to competing interactions and frustration even in the homometallic, nondisordered systems. $Co_5Ti(O_2BO_3)_2$ is distinguished among the magnetic ludwigites we have studied by having the largest γ value, which is consistent with the spin-glass nature of its low-temperature magnetic state.[21] In Table V we can see that the magnetic field quenches substantially the linear temperature-dependent specific-heat term confirming the magnetic character of the modes which give rise to this contribution. As in structural glasses these are most probably local configurational modes, in this case magnetic two-level systems with a broad distribution of parameters associated here with different local spin arrangements.

Figure 7 shows the specific heat of $Co_5Ti(O_2BO_3)_2$ for different applied magnetic fields. In the inset of this figure it is plotted the difference between the specific heat at zero and finite magnetic fields. The decrease in $(C/T)_H-(C/T)_{H=0}$ at low temperatures is due to the quenching of the low-energy magnetic modes as we pointed out before. However, as temperature increases this difference becomes null and eventually changes sign. The latter result indicates that the magnetic field has a disruptive effect in the spin-glass ordering increasing the magnetic fluctuations which contribute to the specific heat.

VI. CONCLUSIONS

The family of magnetic oxyborates known as ludwigites constitute an interesting class of materials with a rich magnetic behavior. These systems have low-dimensional subunits in their structure, which are responsible for many of their interesting properties. In spite of the competing interactions arising from different paths for superexchange and intrinsic disorder these systems show long-range magnetic order at low temperatures. The exception is the $Co_5Ti(O_2BO_3)_2$ investigated here where one of the constituent transition metals is in a nonmagnetic state. This material turns out to be a spin glass with a freezing temperature $T_g\approx 19$ K. When

compared with the other ludwigites this is a soft material from the magnetic and structural point of view as is clearly shown by its very large specific heat. This material has a hard axis of magnetization which corresponds to the direction of the ladders. In the plane *ab*, perpendicular to this axis there is a negligible magnetic anisotropy. At low temperatures and zero external magnetic field there is a freezing of the Co moments in random directions in this plane. A small external field, however, can easily orient the magnetic moments in this easy plane. We hope this study will motivate further work in this interesting family of magnetic oxyborates.

ACKNOWLEDGMENTS

Support from the Brazilian agencies CNPq and FAPERJ is gratefully acknowledged.

*mucio@if.uff.br

[1] D. C. Freitas, M. A. Continentino, R. B. Guimarães, J. C. Fernandes, J. Ellena, and L. Ghivelder, Phys. Rev. B **77**, 184422 (2008).
[2] N. B. Ivanova, A. D. Vasiliév, D. A. Velikanov, N. V. Kazak, S. G. Ovchinnikov, G. A. Petrakovskii, and V. V. Rudenko, Phys. Solid State **49**, 651 (2007).
[3] D. C. Freitas, M. A. Continentino, R. B. Guimarães, J. C. Fernandes, E. P. Oliveira, R. E. Santelli, J. Ellena, G. G. Eslava, and L. Ghivelder, Phys. Rev. B **79**, 134437 (2009).
[4] N. V. Kazak, N. B. Ivanova, V. V. Rudenko, A. D. Vasil'ev, D. A. Velikanov, and S. G. Ovchinnikov, Phys. Solid State **51**, 966 (2009).
[5] R. B. Guimarães, M. Mir, J. C. Fernandes, M. A. Continentino, H. A. Borges, G. Cernicchiaro, M. B. Fontes, D. R. S. Candela, and E. Baggio-Saitovich, Phys. Rev. B **60**, 6617 (1999).
[6] J. C. Fernandes, R. B. Guimarães, M. A. Continentino, L. Ghivelder, and R. S. Freitas, Phys. Rev. B **61**, R850 (2000).
[7] M. Mir, R. B. Guimarães, J. C. Fernandes, M. A. Continentino, A. C. Doriguetto, Y. P. Mascarenhas, J. Ellena, E. E. Castellano, R. S. Freitas, and L. Ghivelder, Phys. Rev. Lett. **87**, 147201 (2001).
[8] A. P. Douvalis, A. Moukarika, T. Bakas, G. Kallias, and V. Papaefthymiou, J. Phys.: Condens. Matter **14**, 3303 (2002).
[9] P. Bordet and E. Suard, Phys. Rev. B **79**, 144408 (2009).
[10] Enraf-Nonius COLLECT, Nonius BV, Delft, The Netherlands (1997–2000).
[11] Z. Otwinowski and W. Minor, in *Methods in Enzymology*, edited by C. W. Carter, Jr. and R. M. Sweet (Academic, New York, 1997), Vol. 276.
[12] P. Coppens, L. Leiserowitz, and D. Rabinovich, Acta Crystallogr. **18**, 1035 (1965).
[13] SHELXS97—Program for Crystal Structure Solution (Release 97–2). G. M. Sheldrick, Institüt für Anorganische Chemie der Universität, Tammanstrasse 4, D-3400 Göttingen, Germany, 1998.
[14] SHELXL97—Program for Crystal Structure Refinement (Release 97–2). G. M. Sheldrick, Institüt für Anorganische Chemie der Universität, Tammanstrasse 4, D-3400 Göttingen, Germany, 1998.
[15] L. J. Farrugia, J. Appl. Crystallogr. **32**, 837 (1999).
[16] G. Bergherhoff, M. Berndt, and K. Brandenburg, J. Res. Natl. Inst. Stand. Technol. **101**, 221 (1996).
[17] A. A. Brovkin, I. V. Rozhdestvenskaya, and E. A. Rykova, Crystallogr. Rep. **47**, 412 (2002).
[18] Th. Armbruster and G. A. Lager, Acta Crystallogr., Sect. C: Cryst. Struct. Commun. **41**, 1400 (1985).
[19] C. G. F. Stenger, G. C. Verschoor, and D. J. W. Ijdo, Mater. Res. Bull. **8**, 1285 (1973).
[20] *International Tables for Crystallography*, edited by Theo Hahn, 5th ed. (Springer, Dordrecht, The Netherlands, 2005), Vol. A, p. 283.
[21] See, K. H. Fischer and J. A. Hertz, *Spin Glasses*, Cambridge Studies in Magnetism Vol. 1 (Cambridge University Press, Cambridge, 1993); Sunil Nair, A. K. Nigam, A. V. Narlikar, D. Prabhakaran, and A. Boothroyd, Phys. Rev. B **74**, 132407 (2006).